Received: 2 March 2022 | Accepted: 18 July 2022

DOI: 10.1111/gcb.16396

Global Change Biology WILEY

RESEARCH ARTICLE

Using the atmospheric CO_2 growth rate to constrain the CO_2 flux from land use and land cover change since 1900

Julia L. Dohner[1] | Benjamin Birner[1] | Armin Schwartzman[2,3] | Julia Pongratz[4,5] | Ralph F. Keeling[1]

[1]Scripps Institution of Oceanography, University of California, San Diego, California, USA

[2]Division of Biostatistics, University of California, San Diego, California, USA

[3]Halıcıoğlu Data Science Institute, University of California, San Diego, California, USA

[4]Department of Geography, Ludwig-Maximilians Universität, München, Germany

[5]Max Planck Institute for Meteorology, Hamburg, Germany

Correspondence
Julia L. Dohner, Scripps Institution of Oceanography, University of California, San Diego, CA, USA.
Email: jdohner@ucsd.edu

Funding information
Eric and Wendy Schmidt, Grant/Award Number: Schmidt Futures; National Aeronautics and Space Administration, Grant/Award Number: NNX17AE74G; National Science Foundation, Grant/Award Number: Graduate Research Fellowship Program

Abstract

We explore the ability of the atmospheric CO_2 record since 1900 to constrain the source of CO_2 from land use and land cover change (hereafter "land use"), taking account of uncertainties in other terms in the global carbon budget. We find that the atmospheric constraint favors land use CO_2 flux estimates with lower decadal variability and can identify potentially erroneous features, such as emission peaks around 1960 and after 2000, in some published estimates. Furthermore, we resolve an offset in the global carbon budget that is most plausibly attributed to the land use flux. This correction shifts the mean land use flux since 1900 across 20 published estimates down by 0.35 PgC year^{-1} to 1.04 ± 0.57 PgC year^{-1}, which is within the range but at the low end of these estimates. We show that the atmospheric CO_2 record can provide insights into the time history of the land use flux that may reduce uncertainty in this term and improve current understanding and projections of the global carbon cycle.

KEYWORDS
atmospheric CO_2, CO_2 growth rate, global carbon budget, global CO_2 fluxes, land use change, terrestrial CO_2 sink

1 | INTRODUCTION

The increase in atmospheric CO_2 since the turn of the 19th century has been driven by anthropogenic emissions from fossil fuel burning and industry (FF, hereafter "fossil emissions") and emissions and removals from land use change (LU, hereafter "land use flux"), including land management and related land cover changes (Friedlingstein et al., 2020). These emissions are offset by natural uptake of CO_2 by the terrestrial biosphere (*B*, hereafter referred to as the "terrestrial sink," for which "natural" is implied) and the ocean (*O*) (Broecker et al., 1979; Siegenthaler & Sarmiento, 1993). The balance of these sources and sinks determines the magnitude of the atmospheric growth rate (AGR):

$$\mathrm{AGR} = \mathrm{FF} + \mathrm{LU} - O - B \quad (1)$$

where all fluxes are in units of PgC year^{-1}, and positive values for each term indicate increasing strength of their source (FF, LU) or sink (*O*, *B*).

The atmospheric CO_2 growth rate is well known from contemporary observations and historical reconstructions (Conway &

Tans, 2009; Keeling et al., 2005; MacFarling Meure et al., 2006). As the best estimated term of Equation (1), the growth rate has been used to constrain the combined land and ocean sinks, treating fossil emissions and land use flux as known (Ballantyne et al., 2012; Joos et al., 1999). This process has also been reversed and used to verify fossil emissions (Francey et al., 2010; Peters et al., 2017). The terrestrial sink (B) has commonly been calculated as a residual (B_{res}, referred to as the "residual terrestrial sink") of the other terms of Equation (1) (Le Quéré et al., 2016). Finally, the AGR has also been used to quantify the land use flux occurring in the 19th century, a time when fossil emissions were small and growing atmospheric CO_2 levels supported the existence of significant emissions from land use (Siegenthaler & Oeschger, 1987; Wilson, 1978; Woodwell et al., 1983). However, the growth rate has not been previously used to constrain the land use flux in the 20th century and later.

The land use flux has been estimated using bookkeeping methods and dynamic global vegetation models (DGVMs) (Figure 1). The bookkeeping approach uses vegetation and soil carbon densities to estimate the flow of carbon between the land and atmosphere in response to inferred and historical occurrences of land use activities. DGVMs simulate effects of both natural and anthropogenic processes (including land use) on terrestrial carbon stocks and compare simulations with and without land use activity to calculate the land use CO_2 flux. At present, estimates of the land use flux vary substantially in magnitude and variability across models, and the flux is overall considered to be uncertain by ~50% (Friedlingstein et al., 2020).

The estimates of the land use flux vary widely across models related to differences in (i) underlying land use reconstructions, (ii) the degree of implementation of land use practices, (iii) definitions of the land use flux, and (iv) modeling parameterizations and process representation (Pongratz et al., 2018): (i) The source and implementation of information on changes in agricultural areas and forest management differ across studies (Friedlingstein et al., 2022) and substantially influence land use flux estimates (Gasser et al., 2020), as does uncertainty in the land use reconstructions themselves (Hartung et al., 2021). (ii) Land use practices (e.g., drainage, shifting cultivation, wood harvest) are implemented by the models to different extents (Arneth et al., 2017) and with varying complexity (Pongratz et al., 2018). (iii) DGVMs typically include synergistic effects between natural environmental changes and land use change in their land use flux estimates, while bookkeeping approaches leave them out (Gasser et al., 2020; Obermeier et al., 2021; Pongratz et al., 2014). (iv) Model parameterizations are often not well constrained by observational data, such that, for example, carbon densities differ substantially across bookkeeping models (Bastos et al., 2021); furthermore, the details of processes underlying a realistic land use description, such as vegetation demography, differ widely across DGVMs (Fisher et al., 2018). These model aspects continue to be improved (Blyth et al., 2021; Pongratz et al., 2018) and observations of proxies relevant to land use emissions, such as fires (van Marle et al., 2022), biomass changes (Xu et al., 2021), or forest loss (Feng et al., 2022) increasingly provide additional ways to evaluate the size and evolution at least of certain components of the land use flux. The AGR could provide an additional top-down, independent constraint on the plausibility of the complete land use flux.

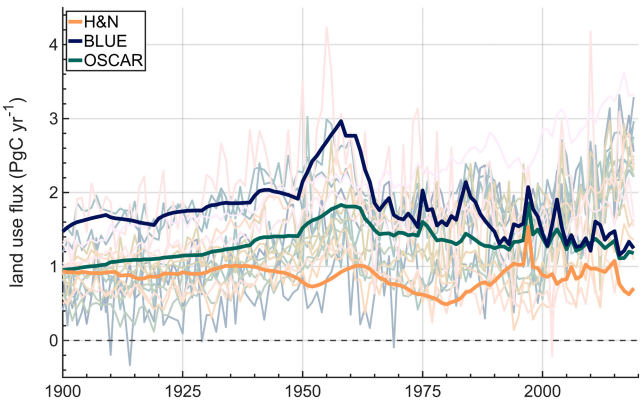

FIGURE 1 Estimates of land use flux via bookkeeping based (H&N, BLUE, OSCAR, in bold) and DGVM-based (17 estimates shown here faintly and separately in Figure S1; see Table S1 for references), all shown at annual resolution. We use the color map batlow (Crameri, 2021) in this study to prevent visual distortion of the data and to make this work accessible to readers with differing color vision (Crameri et al., 2020).

The land use flux has been difficult to characterize and is a primary source of uncertainty in global anthropogenic fluxes of CO_2 (Riahi et al., 2022). Current estimates of land use fluxes have means over 1900–2019 ranging from 0.76 (Vuichard et al., 2019) to 2.15 PgC year^{-1} (Yue & Unger, 2015), with Friedlingstein et al. (2022) reporting an average annual flux of 1.32 ± 0.7 PgC year^{-1} since 1900. Booth et al. (2017) show that reducing uncertainty in the land use flux can substantially narrow the range in projected future climate scenarios, which hinge on models tuned to match past fluxes. Additional constraints are needed to refine estimates of the land use flux and improve projections of the carbon cycle.

Here we examine whether the atmospheric CO_2 growth rate in Equation (1) can be used to constrain the land use flux since 1900. Recognizing that the overall uncertainty in the global carbon budget complicates analysis of land use fluxes on timescales shorter than decadal, we examine to what extent variations in the atmospheric CO_2 growth rate constrain the magnitude of decade-to-decade variability in the land use flux. We address this question by evaluating the compatibility of published estimates of the land use flux with the other terms in Equation (1) via linear regression fits. We examine the distributions of scalars and error in these fits to draw inferences about deficiencies in the prior estimates of the land use flux. In total, we find that the CO_2 growth rate favors land use flux estimates with lower decadal variability, and also find that the budget requires an additive adjustment, which we argue is most plausibly attributed to the land use flux.

2 | METHODS

2.1 | Model optimization

To evaluate the compatibility of various land use flux reconstructions (LU_j) with the AGR, we employ Equation (1) as a linear regression:

TABLE 1 Expressions for generating temporally autocorrelated noise to account for uncertainty in the model inputs CO_2 (atmospheric CO_2 record, used to calculate AGR), FF, and *O*

Term	AR1	AR2	σ	Source
CO_2	0.244	0.086	0.51 PgC	Ballantyne et al. (2012)
FF	0.95	-	5%	Ballantyne et al. (2015)
O	0.9	-	0.4 PgC year^{-1}	Anderegg et al. (2015)

Note: The standard deviation of the generated noise time series is normalized to match published values (σ). Noise in FF is scaled at each yearly value to a standard deviation of 5% of the emissions in that year.

$$\mathrm{AGR} + O - \mathrm{FF} = \mathrm{LU}_j + \alpha - \beta \cdot B_k + \mathrm{error} \quad (2)$$

where subscripts *j* and *k* refer to prior estimates of the land use flux and terrestrial sink, respectively, as compiled by the Global Carbon Project (Friedlingstein et al., 2020), and AGR, *O*, and FF are composite best estimates (Friedlingstein et al., 2020), with noise added, as discussed in Section 2.3. The parameters α and β are scalars fitted to minimize the mean squared error (MSE):

$$\mathrm{MSE} = \frac{1}{(t_1 - t_0) + 1} \sum_{t_0}^{t_1} \left(\overline{\mathrm{error}(t)}\right)^2 \quad (3)$$

where $\overline{\mathrm{error}}$ denotes the error smoothed with a 10-year moving average, and the MSE is calculated over the fitting period in which t_0 is either 1900 or 1959 and t_1 is 2019. The 1900 start was chosen, as opposed to, for example, 1800, to avoid the need to taper the fitted constant α (all terms in the budget were zero prior to the industrial revolution). The 1959 start was chosen to restrict the analysis to the period of direct atmospheric measurements (as opposed to including ice core measurements). The decadal smoothing ensures that emphasis is placed on the decadal and longer timescales that are resolved in the land use flux reconstructions. The decadal smoothing also has the effect of smoothing discontinuities and changes in interannual variability in datasets due to changes in sampling methodology (e.g., atmospheric CO_2 data). The optimized values for α and β depend on the selected prior estimates for the input terms, including LU and B (i.e., $\alpha = \alpha_{jk}$, $\beta = \beta_{jk}$). Below, we report the error alternately as MSE or as the root mean squared error (RMSE = $\sqrt{\mathrm{MSE}}$).

2.2 | Data description

We select LU_j from 20 published land use flux inputs and one hypothetical case of a constant LU. These include three bookkeeping-based estimates from Houghton and Nassikas (2017) (hereafter H&N), the Bookkeeping Land Use Emissions model (BLUE) (Hansis et al., 2015), and OSCAR (Gasser et al., 2020) (all in the updated versions as reported in Friedlingstein et al. (2022)), and 17 DGVM estimates included in Friedlingstein et al. (2020). We also explore a case in which the land use flux is held constant (CONST) over the entire 1900–2019 period, which is equivalent to setting $\mathrm{LU}_j = 0$ because Equation (2) already contains the additive constant α.

For the terrestrial CO_2 sink, we select B_k from 17 DGVM estimates included in Friedlingstein et al. (2020). For the atmospheric CO_2 growth rate, we calculate the growth rate from the monthly atmospheric CO_2 record compiled by Joos and Spahni (2008, updated), which combines atmospheric data from the NOAA/ESRL global network (1980–2019) and Mauna Loa, Hawaii (1958–1979), and ice core data from Law Dome, Antarctica (1600–1957). We use annual global estimates of the ocean sink and CO_2 emissions from fossil fuel burning and industry (including the cement carbonation sink) as put forth by Friedlingstein et al. (2020).

2.3 | Accounting for uncertainty in budget terms

In assessing each land use flux estimate via Equation (2), we apply randomly generated temporally autoregressive noise to the atmospheric CO_2 record (used to calculate AGR), FF, and *O* to allow for uncertainty in these inputs. The autoregressive noise $x_{(t)}$ is produced using the following construction:

$$x_{(t)} = \mathrm{AR1} \cdot x_{(t-1)} + \mathrm{AR2} \cdot x_{(t-2)} + C_1 \cdot \varepsilon_{(t)} \quad (4)$$

where AR1 and AR2 represent the lag 1 and lag 2 autoregressive coefficients, $C_1 = \sqrt{1 - \mathrm{AR1}^2 - \mathrm{AR2}^2}$ represents a scaling factor that normalizes the standard deviation of $x_{(t)}$ to 1, and ε is a Gaussian random variable with mean of 0 and standard deviation of 1. Once calculated, $x_{(t)}$ is scaled to have a standard deviation matching the published decadal uncertainty σ. The specific values used for each of the carbon budget terms are detailed in Table 1. This overall approach follows the "el camino" method described in Ballantyne et al. (2015). Autoregressive errors in FF and *B* are adopted directly from Ballantyne et al. (2015) and Anderegg et al. (2015). The autoregressive error in CO_2 after 1958 is based on Ballantyne et al. (2012).

To account for errors in the atmospheric CO_2 record before 1958, we construct 10,000 bootstrap simulations of the ice core CO_2 data between 1600 and 1957. To construct one bootstrapped time series, from the observed 79-point ice core record time series spanning 1600–1957 we randomly sample with replacement 79 data points with their associated timestamps. This process is repeated 10,000 times. The bootstrap simulations are then joined with the direct atmospheric CO_2 measurements for 1958–2019 and together fit with a smoothing spline. The time series are joined before the spline to ensure continuity between the ice core and atmospheric records. For each of the 10,000 time series, we use a smoothing spline with a cutoff period of 7.6 years for the ice core

data and 2 years for the atmospheric measurements (λ = 25.66, 1-month data spacing, weights of 1 and 0.069 for ice core and atmospheric data, respectively. Parameters are chosen to obtain the desired approximate cutoff periods) (Bruno & Joos, 1997; Enting, 1987). We opt for a relatively low cutoff period for the ice core data as a conservative application of uncertainty. Finally, we truncate each of the 10,000 bootstrapped and spline-fit time series to the years 1900–1957. One of each of these 10,000 time series is joined with one generation of the CO_2 record 1958 and later which includes random temporally autoregressive noise. We then differentiate this joined CO_2 record to calculate the annual AGR centered on July 1 for each model run. This process is repeated for each bootstrapped CO_2 simulation for data prior to 1958 to produce 10,000 instances of the AGR.

We allow for uncertainty in the terrestrial CO_2 sink via bootstrap by randomly choosing with replacement one of 17 DGVM estimates (B_k) in Friedlingstein et al. (2020) for each of the 10,000 ensemble runs. We include multiple formulations of the terrestrial sink rather than applying autoregressive random noise to a central estimate to better allow for systematic bias.

Finally, the distribution of error (Equation 2) for each land use flux estimate LU_j is modeled by creating a 10,000-member ensemble, each member of which includes one pick B_k and one rendering of each of the autoregressive functions and bootstraps. Each land use flux and each ensemble member therein yield a different estimate of the parameters α and β and quality of fit. No special significance is attached to pairs of LU_j and B_k taken from the same DGVM (i.e., $j = k$). The spread in the 17 inputs for B_k and 10,000 instances of AGR, FF, and O are shown in Figure S2.

3 | RESULTS AND DISCUSSION

3.1 | Constraints on decadal variability in land use flux

We find that land use flux estimates with greater decadal variability yield larger errors in Equation (2) for both the 1900–2019 and 1959–2019 timeframes (Figure 2). The model errors increase approximately linearly with the variance in the land use flux input. This relationship appears in both fitting timeframes, with the 1959–2019 period showing a tighter relationship and a greater increase in error per increase in variance than fits over 1900–2019.

To illustrate differences in quality of fit, we examine the RMSE across the 10,000-member ensembles for three land use cases: H&N, BLUE, and CONST. H&N and BLUE are chosen because they make up two of the three estimates that are averaged to report the global land use flux in the Global Carbon Project, and out of these three estimates represent the high- and low-variance endmembers (Figure 1). We also examine the constant land use flux scenario because of its consistently low errors.

As shown in Figure 3, we find that using CONST and H&N leads to similar distributions of RMSE with means of 0.50 and 0.52 PgC year^{-1} respectively, while BLUE yields a higher average

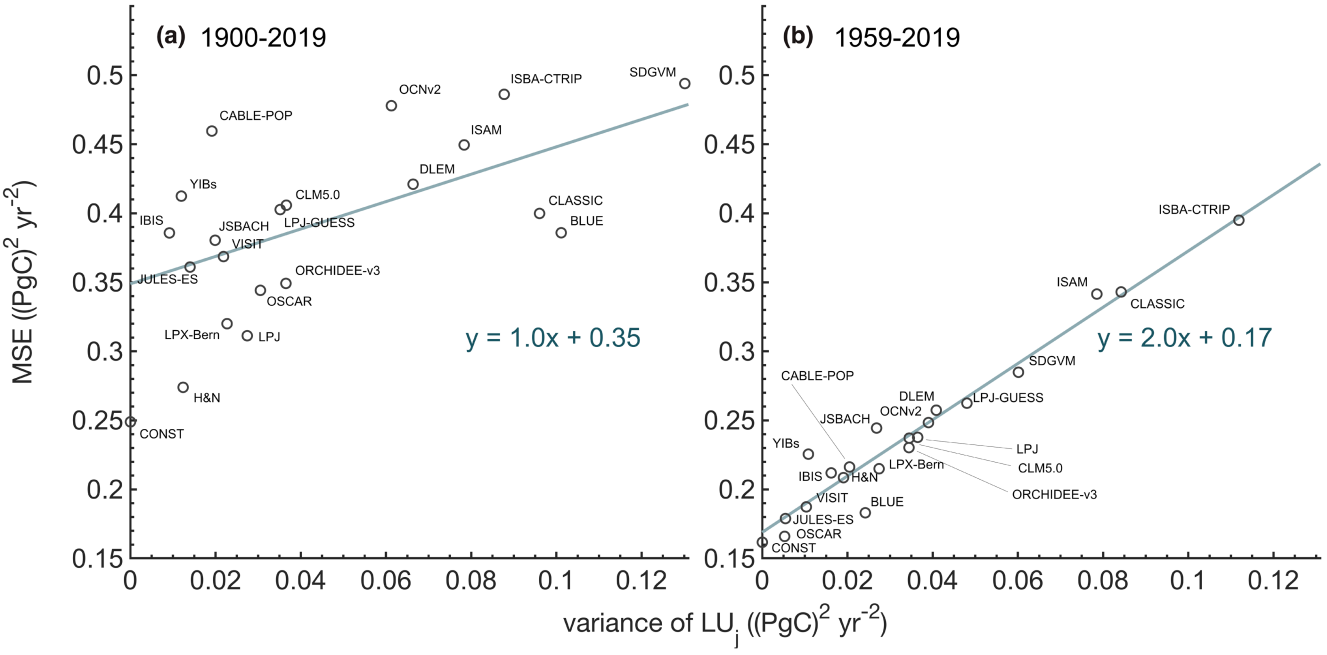

FIGURE 2 Relationship between regression errors in Equation (2) and decadal variability in the land use flux LU_j used as input, with separate analyses for the 1900–2019 (panel [a]) and 1959–2019 (panel [b]) timeframes. The decadal variability in the land use flux is represented as the variance of the decadally smoothed land use flux over each period after removing a linear trend, and the model errors are shown as the mean annual mean squared error (MSE) over the same period across each land use flux's 10,000-member ensemble. The lines and accompanying equations are a linear least-squares fit to the data excluding CONST. All reported data for the grouped land use fluxes hereafter exclude model runs for the CONST case.

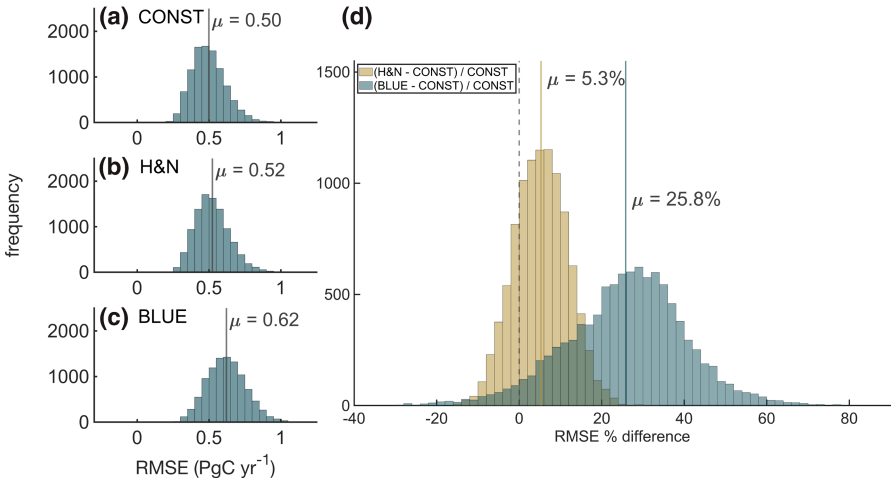

FIGURE 3 Panels (a-c) show the distributions of 10,000-member ensemble error (Equation 3) for runs using CONST, H&N, or BLUE as input for the land use flux over 1900–2019. Panel [d] shows the distributions of the percent differences in error from the 10,000-member ensembles using H&N or BLUE as input for the land use flux compared to the error when using CONST for each member of the ensemble. Ensemble errors are shown as the root mean squared error (RMSE). The interquartile range for the H&N distribution in panel (d) is 9.1% and for the BLUE distribution in panel (d) 18.3%. The dashed vertical line in panel [d] marks zero percent difference, and for all panels the solid vertical lines mark the mean (μ) of each distribution. We hereafter report and discuss results for the 1900–2019 fitting period by default unless otherwise specified.

error of 0.62 PgC year^{-1}. Figure 3d shows the same information, but after calculating the percent difference in RMSE between H&N and CONST or BLUE and CONST on a point-by-point basis through the ensemble (i.e., for identical picks for B_k and time series of noise in AGR, O, and FF). This shows that the RMSE for H&N and BLUE are both systematically higher than that for CONST, with a larger difference for BLUE. The RMSE for the CONST ensemble is lower than the RMSE for any of the published estimates. The model errors for all 21 land use flux cases are listed in Table S1.

The strong correlation between average regression error and decadal variability in land use fluxes can be understood by examining their time histories (Figure 4). We focus again on H&N, BLUE, CONST, and additionally ISBA-CTRIP as a representative high-variance DGVM estimate. The errors of BLUE and ISBA-CTRIP both show a prominent positive excursion in the late 1950s, which coincides with a large variation in the BLUE and ISBA-CTRIP fluxes over the same period. The model errors for CONST and H&N are smaller and generally similar to one another, showing an overestimation of atmospheric growth around 1950 and in the mid-2000s. The mid-2000s error also appears in the ISBA-CTRIP error time series.

The compatibility of land use fluxes with the atmospheric CO_2 growth rate can also be examined in relation to the residual terrestrial sink that is required to balance the global budget ($B_{res} = FF + LU_j - O - AGR$). As shown in Figure 5, the residual sink demanded by BLUE strengthens rapidly from 1920 to 1960, then reverses trajectory and weakens until 1980. This behavior deviates qualitatively from the multi-model mean (B_{GCP}) reported by Friedlingstein et al. (2020) (shown in pink), which increases more uniformly with time. In contrast to BLUE, the terrestrial sink calculated from CONST grows more uniformly after 1900 with smaller decadal variations, leading to a residual terrestrial sink that also grows relatively uniformly with time, in better agreement with models.

The features contributing to error in the higher variability land use flux estimates may be tied to known issues with the methodology used to produce these estimates. In the case of the BLUE and ISBA-CTRIP land use fluxes, for example, the strong land use flux peak around 1960 and the corresponding errors (Figure 4c,d) coincide with changes in the datasets used as inputs before and after 1961. The DGVMs, BLUE, and part of the simulations underlying OSCAR use the harmonized land use change data LUH2 (Chini et al., 2021; Hurtt et al., 2020), which is based on the HYDE population and land use dataset (Goldewijk, Beusen, et al., 2017; Goldewijk, Dekker, et al., 2017). HYDE transforms the country-level statistics on agricultural areas from the Forest and Agriculture Organization (FAO, FAOSTAT, 2021) into spatially explicit maps using ancillary data from satellite remote sensing and rules on how agricultural land is distributed at the sub-national level. Since the FAO estimates only begin in 1961, agricultural areas for earlier time periods are approximated by combining population estimates with per capita land use estimates that follow a curved trajectory based on the (limited) available historical sources. This switch in methodology in 1961 is the likely cause of the high land use flux prior to the 1960s and the subsequent drop (Bastos et al., 2021). The quickening growth in the land use flux between 1940 and 1960 may also be connected to a misrepresentation in the construction of these fluxes. There is evidence that LUH2, which underlies BLUE and DGVM-based estimates including ISBA-CTRIP, does not accurately capture the increase in terrestrial CO_2 uptake associated with land abandonment occurring in the former Soviet Union during the 1940s (Bastos et al., 2016), causing flux estimates to be artificially high during this period.

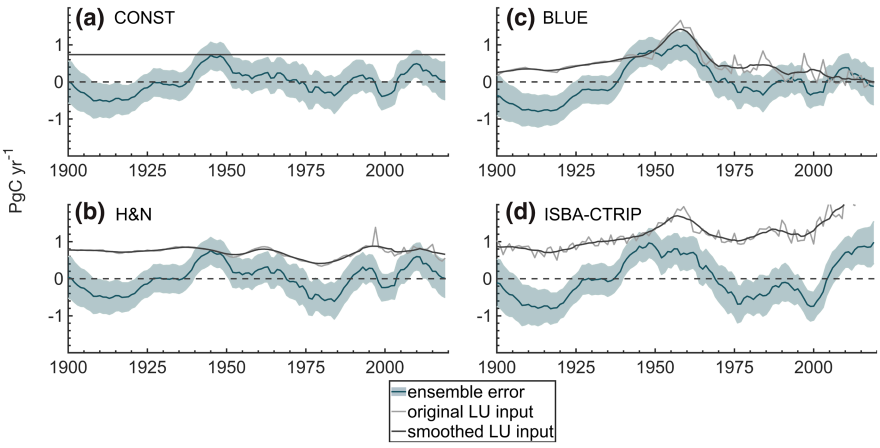

FIGURE 4 Comparison of averaged ensemble error (dark teal) for each land use flux ([a] CONST, [b] H&N, [c] BLUE, and [d] ISBA-CTRIP), shown with an error envelope ($\pm 1\sigma$) in lighter teal. The land use flux (LU), which has been adjusted by the ensemble-averaged fitting parameter α, is shown both in the 10-year smoothed (dark grey) and unsmoothed (light grey) forms.

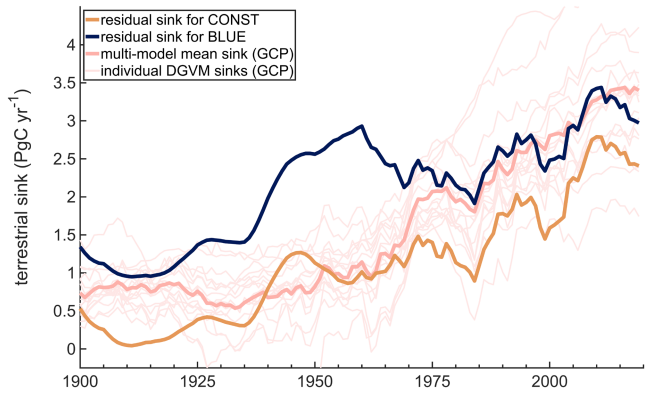

FIGURE 5 Comparisons of terrestrial sink estimates, including sinks inferred as the residual of Equation (1) (B_{res}) assuming different estimates for LU_j where $B_{res} = FF + LU_j - O - AGR$, where LU_j is either CONST or BLUE. Thin pink lines represent estimates of individual models of B per Friedlingstein et al. (2020). No adjustment is made to the means of the land use fluxes in this figure. All data have 10-year smoothing applied.

The upswing and corresponding errors in Figure 4 for ISBA-CTRIP in recent decades are probably unrelated to a concurrent switch in accounting in the underlying dataset HYDE. The HYDE dataset switches from using only decadal to using annual data in 2000, and the consequently higher interannual variability may have increased emissions due to the asymmetry of decay and regrowth (Friedlingstein et al., 2022) and may be a reason for the higher errors in the last decades. However, this switch in accounting applies also to BLUE, which relies on the HYDE dataset but does not show signs of greater error in recent decades, suggesting that the switch to annual data may not be responsible for the upswing seen in DGVMs.

The errors in Figure 4 for ISBA-CTRIP since 2000 may instead be explained by biases in deforestation rates in the LUH2 dataset (Bastos et al., 2020). These biases have been corrected in subsequent versions (Chini et al., 2021). Therefore, the ISBA-CTRIP estimate we use (from Friedlingstein et al. (2020)) is still subject to these biases, but the BLUE estimate (from Friedlingstein et al. (2022)) is not. The post-2000 increase in the ISBA-CTRIP land use flux estimate may also be exacerbated by the inclusion of "loss of additional sink capacity" (discussed in Section 3.2.1), which reinforces increases in the land use flux and is not represented in bookkeeping-based estimates. Overall, these connections between the errors in land use flux estimates and their methodologies illustrate the process by which the atmospheric CO_2 growth rate's constraint on decadal variability may be used to diagnose underlying issues in land use flux estimates.

3.2 | Constraint on the mean land use flux

3.2.1 | Additive parameter α

Information on model performance is also contained in the distribution of the parameter α. Figure 6 shows histograms of α across the full ensemble of land use models for both time periods. We find that the distributions span zero, with a mean value below zero for both time periods. We also find that α is strongly correlated with the time-averaged land use flux estimates used for each fit, with an especially strong correlation for the full 1900–2019 period (Figure 6a and Table 2).

What significance is implied by the distributions of α centering below zero? To address this question, we start with the hypothesis that the ensemble of estimates of the different budget terms, including the model-to-model variations in the published estimates of LU and B, reflect purely random variations around the unknown "true" historical evolution of each of those quantities. If this hypothesis were true, then the distribution of α values associated with the 20 LU model estimates would be expected to have a mean of zero. (This expectation is supported by additional runs using a hypothetical atmospheric record produced via forward runs driven by the ensemble mean estimates for the budget terms. Method and results are detailed in SI.) In contrast, the mean of α across the 20 models (histograms in Figure 6) differs from zero by ~2 times the standard error on both timeframes (SE = std(α)/sqrt(20-1) = 0.16 PgC year^{-1} for 1900–2019 and SE = 0.26 PgC year^{-1} for 1959–2019; distributions shown in Figure 6 histograms). We calculate the standard error using 19 degrees of freedom, conservatively treating the 20 different land use cases as the only varying parameters between runs.

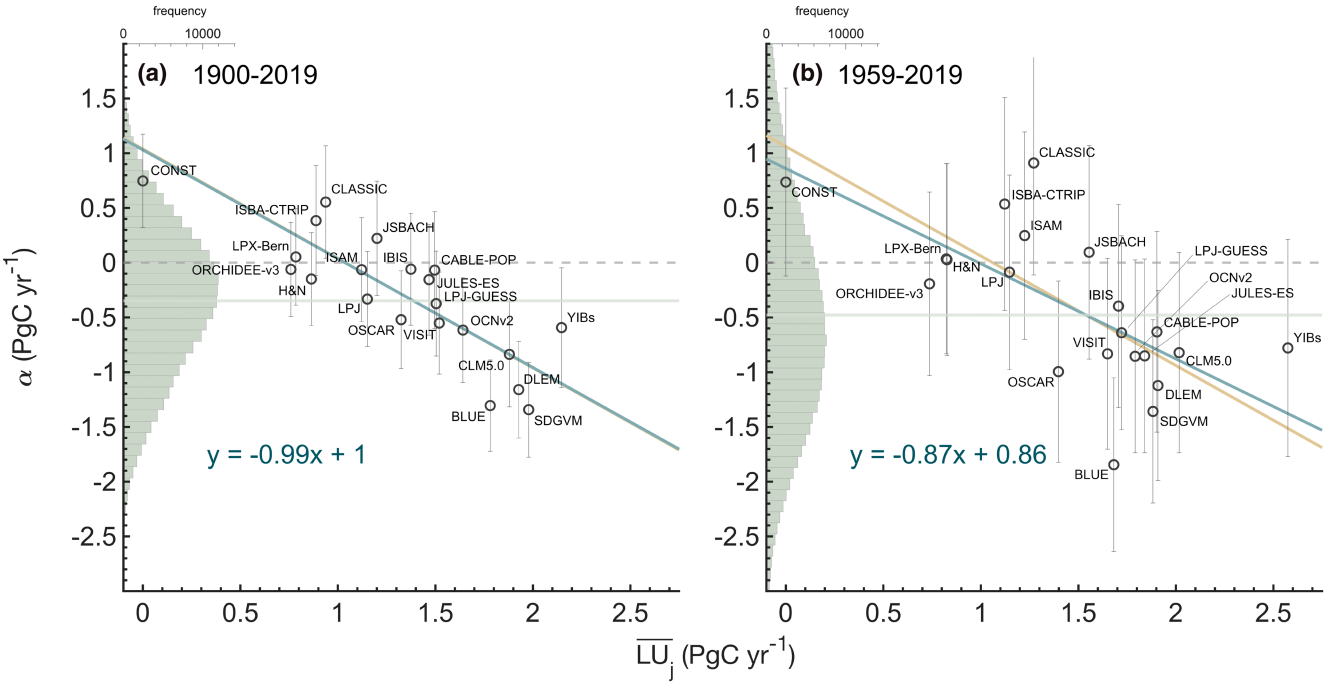

FIGURE 6 Comparison of the ensemble-averaged best fit of additive parameter α (Equation 2) and the time average of the land use flux specified in the ensemble (LU_j), fit and calculated over the 1900–2019 (panel [a]) and 1959–2019 (panel [b]) periods. Points are shown with ±1 standard deviation of the value for α in each LU_j ensemble. The time average of LU_j (denoted as $\overline{LU_j}$) is calculated after applying 10-year smoothing. The teal lines and accompanying equations are a linear least-squares fit to the data, whereas the gold lines are fits to the data with slopes equal to unity (the gold line is obscured by the teal line in panel [a]). Also shown are histograms of the model-fitted values of α across the 20×10,000 ensemble runs for each fitting period (panel [a]: $\mu = -0.35 \pm 0.70$; panel [b]: $\mu = -0.48 \pm 1.11$). Zero is marked with a dashed line and the histogram means are marked with a solid line that extends into the scatter. The ensemble means of $\overline{LU_j} + \alpha$ for each time period can be inferred from the projection onto the x-axis of the intersection point of the gold line (slope = 1, line of constant $\overline{LU_j} + \alpha$) and the zero line.

TABLE 2 Correlation coefficients and *p*-values of the relationship between (i) the means of fitting parameters α and β across ensemble runs specific to each model input and (ii) means of model inputs of the land use flux ($\overline{LU_j}$, where overbar denotes the time average) and terrestrial sink ($\overline{B_k}$)

		$\overline{LU_j}$		$\overline{B_k}$	
		1900–2019	**1959–2019**	**1900–2019**	**1959–2019**
α	Correlation coefficient	−0.80	−0.60	0.46	0.12
	p-value	2.5×10^{-5}	0.0049	0.060	0.64
β	Correlation coefficient	0.0071	0.11	−0.56	−0.62
	p-value	0.98	0.63	0.021	0.0083

Note: For example, values of α found when using each of the 20 inputs for LU are compared to the means of the respective LU, with the fits performed over the 1900–2019 fitting timeframe and $\overline{LU_j}$ calculated over 1900–2019, in the case of the 1900–2019 column. *p*-values are calculated using the MATLAB *corrcoef* function. Model inputs LU_j are assumed to be independent, as are B_k (discussed above). Scatterplots of these data are embedded in Figure 6 and displayed in isolation in SI (Figures S6 and S7).

Thus, we are able to falsify the hypothesis. Of course, one might argue that the hypothesis was anyway doubtful because the different models for LU and *B* share assumptions, methods and input datasets. Nevertheless, our ability to falsify the hypothesis using atmospheric data has broader implications, because it provides a means to identify a specific bias that was previously not recognized.

How should we interpret the strong correlation between α and the mean land use fluxes across the 20-model ensemble? We argue that this correlation suggests that α is best interpreted as a correction to the budget imbalance involving LU. This interpretation is supported by the following points: First, the range in α is larger than the uncertainties in AGR, FF, and O, so α cannot be significantly associated with errors in these terms. Second, a similarly strong correlation as that between α and the mean land use flux is not found between α and the mean land sink *B* over either the 1900–2019 or 1959–2019 periods (correlations shown in Table 2; Figures S6 and S7). Third,

TABLE 3 Average values of $\overline{LU_j} + \alpha$, where α is the ensemble-averaged best fit additive parameter and $\overline{LU_j}$ is the mean across all 20 land use flux cases

	$\overline{LU_j} + \alpha$	
	1900–2019	1959–2019
All LU cases, unweighted	1.04 ± 0.57	1.06 ± 1.04
All LU cases, weighted by 1/MSE	1.06 ± 0.56	0.98 ± 1.03
CONST	0.75 ± 0.43	0.74 ± 0.86
Average of 20 LU cases used in this study (Figure 1)	1.39 ± 0.7	1.54 ± 0.7
Friedlingstein et al. (2022)	1.32 ± 0.7	1.30 ± 0.7

Note: The averages comprise individual ensemble fits of $\overline{LU_j} + \alpha$ for each land use case in the grouping (e.g., 20 LU cases × 10,000 runs = 200,000 ensemble runs for "All LU cases"). "All LU cases" does not include the ensemble runs for the hypothetical constant land use case CONST. Average values of $\overline{LU_j} + \alpha$ are compared to published estimates (bottom two rows). All data are in PgC year^{-1}.

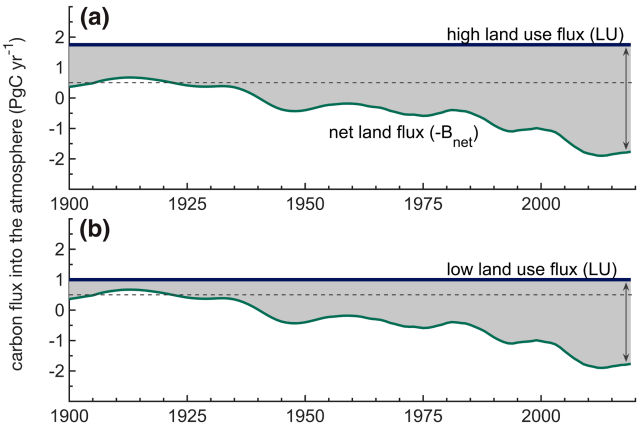

FIGURE 7 The residual terrestrial sink (shaded grey) given two land use flux scenarios with different 1900–2019 means. The residual sink is calculated as the difference between LU (blue line, 1.75 PgC year^{-1} in panel [a] and 1 PgC year^{-1} in panel [b]) and the budget-constrained sign-reversed residual net land flux B_{net} = FF − AGR − O (green curve). The mean 1900–1910 net land flux is marked with a dashed grey line to highlight the relative growth in B_{res} between 1900 and 2019.

interpreting α as a correction to B would significantly change the time evolution of B by reducing its relative growth since 1900 (discussed further below). However, adjusting LU by α does not have this effect, and the offset in α is similar in magnitude to differences in published mean values of LU.

We thus proceed with the assumption that $\overline{LU_j} + \alpha$ can be interpreted as an adjusted estimate of the land use flux mean $\overline{LU_j}$, and report the adjusted flux both for (i) values of α estimated for individual land use cases and (ii) when averaging $\overline{LU_j} + \alpha$ across the 20-model ensemble. For each land use flux case LU_j, we calculate α as the average value across the 10,000 model runs. The resulting $\overline{LU_j} + \alpha$ value for each land use flux case is lower than $\overline{LU_j}$ in the majority of cases (Figure 6 and Table S1). Averaging $\overline{LU_j} + \alpha$ across land use flux cases yields values that are consistently lower than the average of the 20 versions of $\overline{LU_j}$ as well as the Friedlingstein et al. (2022) estimate (Table 3), which is an average of the three bookkeeping estimates H&N, BLUE, and OSCAR. These adjusted land use flux estimates are robust to the details of averaging. An unweighted average of the adjusted land use flux across the 20-model ensemble (excluding CONST) yields 1.04 ± 0.57 PgC year^{-1} when optimizing over 1900–2019 and 1.06 ± 1.04 PgC year^{-1} when optimizing over 1959–2019 (Table 3). Weighting inversely with model error (MSE) yields 1.06 ± 0.56 PgC year^{-1} and 0.98 ± 1.03 PgC year^{-1} when optimizing over 1900–2019 and 1959–2019, respectively. The corresponding estimate for the CONST scenario (for which $\overline{LU_j} = 0$) yields 0.75 ± 0.43 PgC year^{-1} and 0.74 ± 0.86 PgC year^{-1} for 1900–2019 and 1959–2019, respectively. For the 1900–2019 period, the spread in $\overline{LU_j} + \alpha$ is reduced below the designated LU uncertainty of 0.7 PgC year^{-1} quoted in Friedlingstein et al. (2022). The 1959–2019 period does not show a reduced spread in $\overline{LU_j} + \alpha$ because the adjustment incorporates uncertainty in the other terms of the budget, particularly fossil fuel emission, which is a large source of uncertainty in recent years.

What aspects of the record yield this emergent constraint on the mean land use flux? To address this point, we consider the simplest case of a constant land use flux, which essentially contains the same constraint. The atmospheric budget tightly constrains the time history of the residual net land flux, B_{net} = FF − AGR − O. With this constraint, the relative growth in the terrestrial sink, calculated as the residual of the budget (B_{res}), is strongly dependent on the constant value assumed for LU. A high value for LU yields much lower relative growth in B_{res} than a low LU mean (Figure 7). A constraint on the relative growth in B, combined with the assumption that LU is relatively constant, is therefore sufficient to constrain LU.

Our ability to constrain the constant α and to interpret this as an adjustment to the mean land use flux is therefore strongly conditioned upon the published estimates of LU and B having distinct temporal patterns, with LU remaining relatively constant over the evaluation periods, and B growing strongly. This aspect of the published estimates is clearly rooted in mechanistic understanding. The land use flux is driven by competing influences that reduce its long-term trend. Although the global population grew fourfold from 1900 to 2019, the relative influence of population on land use is largely offset by changes in technology (Goldewijk, 2001; Meyer & Turner, 1992), such as the advent of industrialized agriculture in the post-war era (Pongratz et al., 2008). Hong et al. (2021) showed that after 1960 substantial growth in population and agricultural production per capita was largely balanced by decreases in land required per unit of agricultural production associated with agricultural intensification. And although rates of tropical deforestation have increased since 1900, their resulting CO_2 emissions have been largely offset by fire suppression and declining deforestation elsewhere along with the resulting drawdown of CO_2 from regrowth in abandoned deforested and agricultural areas (Houghton et al., 2012).

In contrast, the known drivers of the terrestrial sink have all accelerated since 1900. Gross primary production, water use efficiency of plants, and biomass production have, all with high confidence,

increased (Walker et al., 2020). Nitrogen deposition is also shown to have increased since 1900 (Ackerman et al., 2019; Galloway & Cowling, 2002), which has enhanced global net primary production (Magnani et al., 2007; Reay et al., 2008). Furthermore, fertilization of the terrestrial biosphere by increasing atmospheric CO_2 concentrations has been repeatedly shown to be a primary driver of the terrestrial CO_2 sink (Ciais et al., 2013; Huntzinger et al., 2017; Piao et al., 2013; Sitch et al., 2008; Walker et al., 2020). While the sensitivities of the terrestrial CO_2 sink to these processes remain uncertain, these processes have all clearly increased since 1900, supporting strong growth in the terrestrial CO_2 sink.

We are aware of at least one driver of LU that may have grown similarly to *B*, that is, the "loss of additional sink capacity" (Pongratz et al., 2014). This flux, which is included in DGVMs but not bookkeeping estimates of the land use flux, represents the lost capacity in the terrestrial sink due to land use and has similar drivers to the terrestrial sink. In our model, such a flux would be attributed to a decline in the strength of the terrestrial sink $\beta \cdot B_k$ (discussed in Section 3.2.2). Although we would expect such a decline to be reflected in our model's terrestrial sink, we do not see an obvious difference in $\beta \cdot B_k$ between models that do (DGVMs) and do not (bookkeeping) include lost sink capacity in the land use flux (Table S1). There is currently no consensus on how to incorporate the loss of additional sink capacity into land use models and this flux is sensitive to the details of the modeling approach (Pongratz et al., 2014).

An important question is whether the atmospheric budget can resolve changes in the land use flux on a broader range of timescales than explored here. Answering this remains difficult because of ambiguity in how to assign model error; while the residual errors in Figure 4 might be due to the land use flux, they might also be due to errors in other terms. In line with this reasoning, our model cannot be inverted to produce an optimized land use flux to a decadal precision better than the RMSE of the CONST land use flux case (±0.5 PgC year^{-1}); we take the RMSE of CONST as an optimistic (lower bound) estimate of decadal model error. Possible decadal changes in the land use flux highlighted in other studies, for example, wartime impacts on land use (Bastos et al., 2018) and interannual changes in deforestation rates (Hansen et al., 2013; Houghton et al., 2012), are therefore not challenged by our results.

3.2.2 | Implications for the terrestrial sink

Although we mainly focus on implications for the land use flux, our method also yields insights on the magnitude of the terrestrial sink, *B*. We interpret β as a corrective scaling factor on the terrestrial sink pick B_k. Across the 20-LU model grouped ensemble fit over 1959–2019, the average value of $\beta \cdot \overline{B_k}$ is 1.99 ± 1.05 PgC year^{-1} over the same period, which is ~15% smaller than the multi-model mean terrestrial sink reported in Friedlingstein et al. (2020) of 2.35 ± 0.60 PgC year^{-1} over the same time period (Table S2). We note, however, that the bias suggested by β is not as strong as that suggested by α. If *B* were unbiased, β would bracket unity. Our model finds values for β of 0.93 ± 0.39 for 1900–2019 and 0.89 ± 0.50 for 1959–2019, which are closer to unity within the standard error (DOF = 19).

3.2.3 | Implications for climate sensitivity

The mean land use flux since 1900 is relevant to metrics of climate sensitivity that hinge on the ratio of observed warming to cumulative emissions, such as the transient climate response to cumulative emissions (TCRE) (Millar & Friedlingstein, 2018). Millar and Friedlingstein use a combination of results by Houghton et al. (2012) and Van Der Werf et al. (2010) as reported by Le Quéré et al. (2016), including a land use flux with a 1900–2016 mean of 1.1 PgC year^{-1} to estimate the TCRE. If we assume the true land use flux is relatively constant and has a 1900–2019 mean of 1.04 PgC year^{-1}, then the cumulative anthropogenic CO_2 emissions (FF + LU) 2016 and prior are reduced by ~4%, corresponding to a 4% increase in the TCRE, implying that future increases in global temperature are underpredicted.

3.2.4 | Implications for airborne fraction

The adjusted land use flux is also relevant to estimating trends in the airborne fraction (AF) of CO_2, defined as the annual increment in atmospheric CO_2 divided by the sum of fossil and land use emissions $\left(\mathrm{AF} = \frac{\mathrm{AGR}}{\mathrm{FF+LU}}\right)$. Canadell et al. (2007) used a land use flux updated from Houghton (2003) with a 1959–2006 mean of 1.15 PgC year^{-1} to suggest that the AF increased by 2.5% per decade over the same period. However, calculating the AF trend across each $\overline{\mathrm{LU}_j} + \alpha$ in the 20-model grouping (fit over 1959–2019, with AF trend fit separately for every instance of LU, α and inputs [n = 200,000]) yields an average trend of −0.03 ± 1.52% per decade over 1959–2019. A diminished trend was supported by Knorr (2009), who noted the AFs sensitivity to the land use flux and estimated the trend at 0.7 ± 1.4% per decade after accounting for uncertainties in the global carbon budget, as well as by van Marle et al. (2022), who use visibility data in forest regions to estimate a new land use flux estimate and report a decrease in AF of 0.014 ± 0.010 decade^{-1} since 1959.

4 | SUMMARY

We show that the observed atmospheric CO_2 growth rate can place meaningful constraints on both the decadal variability and mean of the land use CO_2 flux since 1900 when accounting for variations in the major sources and sinks of CO_2 to the atmosphere. We use estimates of the atmospheric CO_2 growth rate, fossil fuel emissions, ocean sink and natural terrestrial sink in a regression in which we alternately use 20 different estimates of the land use flux. We compare the magnitude and timing of the regression errors when using each land use flux input, as well as examine the significance of the regression fitting parameters.

We find that the observed atmospheric CO_2 growth rate since 1900 is better simulated using land use flux estimates with less decadal variability, and the error in simulating the AGR increases roughly in proportion to the amount of decadal variability in the land use flux. The land use flux estimates have coincident features of variability and error between mid-century that may be the result of issues in the underlying datasets. Most DGVM-based land use flux estimates include large errors after 2000, which also point to potential errors in the inputs common to these estimates. We find that a scenario that assumes the land use flux is constant after 1900 matches the atmospheric CO_2 growth rate better than any previously published estimate, even after allowing a constant additive adjustment to the published estimates.

Our model resolves a budget adjustment that is on average negative and which we interpret as a correction to the mean of published land use fluxes, one of the least well-known components of the global carbon budget. This interpretation is based on the additive correction being strongly correlated with the average land use flux over the last century from different LU estimates but not with the terrestrial sink or other terms in the carbon budget. If we alternately interpret the additive constant as a correction to the terrestrial sink, this greatly reduces the relative growth of the sink since 1900, which is inconsistent with the relative growth of published estimates, as rooted in mechanistic understanding.

Interpreting the additive constant as a correction to the mean land use flux yields an atmospherically adjusted mean land use flux of 1.04 ± 0.57 PgC year^{-1} over 1900–2019 and 1.06 ± 1.04 PgC year^{-1} over 1959–2019. These adjusted values are at the low end of the distribution of published estimates. The downward adjustment to the mean land use flux requires a ~15% reduction in the strength of the natural terrestrial sink over 1959–2019 compared to the multi-model mean published by GCP (Friedlingstein et al., 2020). In all, we find that the atmospheric CO_2 budget favors land use flux estimates with less decadal variability and may resolve an overall downward adjustment to the mean land use flux since 1900.

ACKNOWLEDGMENTS

This work was supported by the National Science Foundation Graduate Research Fellowship Program, by NASA under grant NNX17AE74G, and by Eric and Wendy Schmidt via recommendation of the Schmidt Futures program.

CONFLICT OF INTEREST

The authors declare no competing interests.

DATA AVAILABILITY STATEMENT

The data that support the findings of this study are available in the public domain: https://www.globalcarbonproject.org/, https://scripps co2.ucsd.edu/, https://gml.noaa.gov/. Data used in this study that are not immediately available online are available at https://doi.org/10.6076/D11G6B.

ORCID

Julia L. Dohner https://orcid.org/0000-0002-6131-3938
Benjamin Birner https://orcid.org/0000-0003-3139-9897
Armin Schwartzman https://orcid.org/0000-0001-5335-1611
Julia Pongratz https://orcid.org/0000-0003-0372-3960
Ralph F. Keeling https://orcid.org/0000-0002-9749-2253

REFERENCES

Ackerman, D., Millet, D. B., & Chen, X. (2019). Global estimates of inorganic nitrogen deposition across four decades. *Global Biogeochemical Cycles*, *33*(1), 100–107. https://doi.org/10.1029/2018GB005990

Anderegg, W. R. L., Ballantyne, A. P., Smith, W. K., Majkut, J., Rabin, S., Beaulieu, C., Birdsey, R., Dunne, J. P., Houghton, R. A., Myneni, R. B., Pan, Y., Sarmiento, J. L., Serota, N., Shevliakova, E., Tans, P., & Pacala, S. W. (2015). Tropical nighttime warming as a dominant driver of variability in the terrestrial carbon sink. *Proceedings of the National Academy of Sciences of the United States of America*, *112*(51), 15591–15596. https://doi.org/10.1073/pnas.1521479112

Arneth, A., Sitch, S., Pongratz, J., Stocker, B. D., Ciais, P., Poulter, B., Bayer, A. D., Bondeau, A., Calle, L., Chini, L. P., Gasser, T., Fader, M., Friedlingstein, P., Kato, E., Li, W., Lindeskog, M., Nabel, J. E. M. S., Pugh, T. A. M., Robertson, E., … Zaehle, S. (2017). Historical carbon dioxide emissions caused by land-use changes are possibly larger than assumed. *Nature Geoscience*, *10*, 79–84. https://doi.org/10.1038/ngeo2882

Ballantyne, A. P., Alden, C. B., Miller, J. B., Tans, P. P., & White, J. W. C. (2012). Increase in observed net carbon dioxide uptake by land and oceans during the past 50 years. *Nature*, *488*, 70–72. https://doi.org/10.1038/nature11299

Ballantyne, A. P., Andres, R., Houghton, R., Stocker, B. D., Wanninkhof, R., Anderegg, W., Cooper, L. A., DeGrandpre, M., Tans, P. P., Miller, J. B., Alden, C., & White, J. W. C. (2015). Audit of the global carbon budget: Estimate errors and their impact on uptake uncertainty. *Biogeosciences*, *12*(8), 2565–2584. https://doi.org/10.5194/bg-12-2565-2015

Bastos, A., Ciais, P., Barichivich, J., Bopp, L., Brovkin, V., Gasser, T., Peng, S., Pongratz, J., Viovy, N., & Trudinger, C. M. (2016). Re-evaluating the 1940s CO_2 plateau. *Biogeosciences*, *13*(17), 4877–4897. https://doi.org/10.5194/bg-13-4877-2016

Bastos, A., Hartung, K., Nützel, T. B., Nabel, J. E. M. S., Houghton, R. A., & Pongratz, J. (2021). Comparison of uncertainties in land use change fluxes from bookkeeping model parameterisation. *Earth System Dynamics*, *12*(2), 745–762. https://doi.org/10.5194/esd-12-745-2021

Bastos, A., O'Sullivan, M., Ciais, P., Makowski, D., Sitch, S., Friedlingstein, P., Chevallier, F., Rödenbeck, C., Pongratz, J., Luijkx, I. T., Patra, P. K., Peylin, P., Canadell, J. G., Lauerwald, R., Li, W., Smith, N. E., Peters, W., Goll, D. S., Jain, A. K., … Zaehle, S. (2020). Sources of uncertainty in regional and global terrestrial CO_2 exchange estimates. *Global Biogeochemical Cycles*, *34*(2), Article e2019GB006393. https://doi.org/10.1029/2019GB006393

Bastos, A., Peregon, A., Gani, É. A., Khudyaev, S., Yue, C., Li, W., Gouveia, C. M., & Ciais, P. (2018). Influence of high-latitude warming and land use changes in the early 20th century northern Eurasian CO_2 sink. *Environmental Research Letters*, *13*, 065014. https://doi.org/10.1088/1748-9326/aac4d3

Blyth, E. M., Arora, V. K., Clark, D. B., Dadson, S. J., De Kauwe, M. G., Lawrence, D. M., Melton, J. R., Pongratz, J., Turton, R. H., Yoshimura, K., & Yuan, H. (2021). Advances in land surface modelling. *Current Climate Change Reports*, *7*, 45–71. https://doi.org/10.1007/s40641-021-00171-5

Booth, B. B. B., Harris, G. R., Murphy, J. M., House, J. I., Jones, C. D., Sexton, D., & Sitch, S. (2017). Narrowing the range of future climate projections

using historical observations of atmospheric CO_2. *Journal of Climate*, *30*(8), 3039–3053. https://doi.org/10.1175/jcli-d-16-0178.1

Broecker, W. S., Takahashi, T., Simpson, H. J., & Peng, T. H. (1979). Fate of fossil fuel carbon dioxide and the global carbon budget. *Science*, *206*(4417), 409–418. https://doi.org/10.1126/science.206.4417.409

Bruno, M., & Joos, F. (1997). Terrestrial carbon storage during the past 200 years: A Monte Carlo analysis of CO_2 data from ice core and atmospheric measurements. *Global Biogeochemical Cycles*, *11*(1), 111–124. https://doi.org/10.1029/96GB03611

Canadell, J. G., Le Quéré, C., Raupach, M. R., Field, C. B., Buitenhuis, E. T., Ciais, P., Conway, T. J., Gillett, N. P., Houghton, R. A., & Marland, G. (2007). Contributions to accelerating atmospheric CO_2 growth from economic activity, carbon intensity, and efficiency of natural sinks. *Proceedings of the National Academy of Sciences of the United States of America*, *104*(47), 18866–18870. https://doi.org/10.1073/pnas.0702737104

Chini, L., Hurtt, G., Sahajpal, R., Frolking, S., Klein Goldewijk, K., Sitch, S., Ganzenmüller, R., Ma, L., Ott, L., Pongratz, J., & Poulter, B. (2021). Land use harmonization datasets for annual global carbon budgets. *Earth System Science Data*, *13*(8), 4175–4189. https://doi.org/10.5194/essd-13-4175-2021

Ciais, P., Sabine, C., Bala, G., Bopp, L., Brovkin, V., Canadell, J., Chhabra, A., DeFries, R., Galloway, J., Heimann, M., Jones, C., Le Quéré, C., Myneni, R. B., Piao, S., & Thornton, P. (2013). Carbon and other biogeochemical cycles. In T. F. Stocker, D. Qin, G.-K. Plattner, M. Tignor, S. K. Allen, J. Boschung, A. Nauels, Y. Xia, V. Bex, & P. M. Midgley (Eds.), *Climate change 2013: The physical science basis. Contribution of Working Group I to the fifth assessment report of the Intergovernmental Panel on Climate Change* (pp. 465–570). Cambridge University Press.

Conway, T., & Tans, P. (2009). *Atmospheric carbon dioxide mixing ratios from the NOAA CMDL carbon cycle cooperative global air sampling network* (2009). (No. NDP-005). Environmental System Science Data Infrastructure for a Virtual Ecosystem (ESS-DIVE), Carbon Dioxide Information Analysis Center (CDIAC) & Oak Ridge National Laboratory (ORNL). https://doi.org/10.3334/CDIAC/ATG.NDP005

Crameri, F. (2021). Scientific colour maps, Version 7.0.1. *Zenodo*. https://doi.org/10.5281/zenodo.5501399

Crameri, F., Shephard, G. E., & Heron, P. J. (2020). The misuse of colour in science communication. *Nature Communications*, *11*, Article 5444. https://doi.org/10.1038/s41467-020-19160-7

Delire, C., Séférian, R., Decharme, B., Alkama, R., Calvet, J.-C., Carrer, D., Gibelin, A.-L., Joetzjer, E., Morel, X., Rocher, M., & Tzanos, D. (2020). The global land carbon cycle simulated with ISBA-CTRIP: Improvements over the last decade. *Journal of Advances in Modeling Earth Systems*, *12*(9), Article e2019MS001886. https://doi.org/10.1029/2019MS001886

Enting, I. G. (1987). On the use of smoothing splines to filter CO_2 data. *Journal of Geophysical Research*, *92*(D9), 10977–10984. https://doi.org/10.1029/JD092iD09p10977

FAOSTAT. (2021). Food and Agriculture Organization Statistics Division, http://faostat.fao.org/

Feng, Y., Zeng, Z., Searchinger, T. D., Ziegler, A. D., Wu, J., Wang, D., He, X., Elsen, P. R., Ciais, P., Xu, R., Guo, Z., Peng, L., Tao, Y., Spracklen, D. V., Holden, J., Liu, X., Zheng, Y., Xu, P., Chen, J., … Zheng, C. (2022). Doubling of annual forest carbon loss over the tropics during the early twenty-first century. *Nature Sustainability*, *5*, 444–451. https://doi.org/10.1038/s41893-022-00854-3

Fisher, R. A., Koven, C. D., Anderegg, W. R. L., Christoffersen, B. O., Dietze, M. C., Farrior, C. E., Holm, J. A., Hurtt, G. C., Knox, R. G., Lawrence, P. J., Lichstein, J. W., Longo, M., Matheny, A. M., Medvigy, D., Muller-Landau, H. C., Powell, T. L., Serbin, S. P., Sato, H., Shuman, J. K., … Moorcroft, P. R. (2018). Vegetation demographics in earth system models: A review of progress and priorities. *Global Change Biology*, *24*(1), 35–54. https://doi.org/10.1111/gcb.13910

Francey, R. J., Trudinger, C. M., Van Der Schoot, M., Krummel, P. B., Steele, L. P., & Langenfelds, R. L. (2010). Differences between trends in atmospheric CO_2 and the reported trends in anthropogenic CO_2 emissions. *Tellus B: Chemical and Physical Meteorology*, *62*(5), 316–328. https://doi.org/10.1111/j.1600-0889.2010.00472.x

Friedlingstein, P., Jones, M. W., O'Sullivan, M., Andrew, R. M., Bakker, D. C. E., Hauck, J., Le Quéré, C., Peters, G. P., Peters, W., Pongratz, J., Sitch, S., Canadell, J. G., Ciais, P., Jackson, R. B., Alin, S. R., Anthoni, P., Bates, N. R., Becker, M., Bellouin, N., … Zeng, J. (2022). Global carbon budget 2021. *Earth System Science Data*, *14*(4), 1917–2005. https://doi.org/10.5194/essd-14-1917-2022

Friedlingstein, P., O'Sullivan, M., Jones, M. W., Andrew, R. M., Hauck, J., Olsen, A., Peters, G. P., Peters, W., Pongratz, J., Sitch, S., Le Quéré, C., Canadell, J. G., Ciais, P., Jackson, R. B., Alin, S., Aragão, L. E. O. C., Arneth, A., Arora, V., Bates, N. R., … Zaehle, S. (2020). Global carbon budget 2020. *Earth System Science Data*, *12*(4), 3269–3340. https://doi.org/10.5194/essd-12-3269-2020

Galloway, J. N., & Cowling, E. B. (2002). Reactive nitrogen and the world: 200 years of change. *Ambio–A Journal of Environment and Society*, *31*(2), 64–71. https://doi.org/10.1579/0044-7447-31.2.64

Gasser, T., Crepin, L. L., Quilcaille, Y., Houghton, R. A., Ciais, P., & Obersteiner, M. (2020). Historical CO_2 emissions from land use and land cover change and their uncertainty. *Biogeosciences*, *17*(15), 4075–4101. https://doi.org/10.5194/bg-17-4075-2020

Goldewijk, K. K. (2001). Estimating global land use change over the past 300 years: The HYDE database. *Global Biogeochemical Cycles*, *15*(2), 417–433. https://doi.org/10.1029/1999GB001232

Goldewijk, K. K., Beusen, A., Doelman, J., & Stehfest, E. (2017). Anthropogenic land use estimates for the Holocene—HYDE 3.2. *Earth System Science Data*, *9*(2), 927–953. https://doi.org/10.5194/essd-9-927-2017

Goldewijk, K. K., Dekker, S. C., & Van Zanden, J. L. (2017). Per-capita estimations of long-term historical land use and the consequences for global change research. *Journal of Land Use Science*, *12*(5), 313–337. https://doi.org/10.1080/1747423X.2017.1354938

Hansen, M. C., Potapov, P. V., Moore, R., Hancher, M., Turubanova, S. A., Tyukavina, A., Thau, D., Stehman, S. V., Goetz, S. J., Loveland, T. R., Kommareddy, A., Egorov, A., Chini, L., Justice, C. O., & Townshend, J. R. G. (2013). High-resolution global maps of 21st-century forest cover change. *Science*, *342*(6160), 850–853. https://doi.org/10.1126/science.1244693

Hansis, E., Davis, S. J., & Pongratz, J. (2015). Relevance of methodological choices for accounting of land use change carbon fluxes. *Global Biogeochemical Cycles*, *29*(8), 1230–1246. https://doi.org/10.1002/2014GB004997

Hartung, K., Bastos, A., Chini, L., Ganzenmüller, R., Havermann, F., Hurtt, G. C., Loughran, T., Nabel, J. E. M. S., Nützel, T., Obermeier, W. A., & Pongratz, J. (2021). Bookkeeping estimates of the net land-use change flux—A sensitivity study with the CMIP6 land-use dataset. *Earth System Dynamics*, *12*(2), 763–782. https://doi.org/10.5194/esd-12-763-2021

Haverd, V., Smith, B., Nieradzik, L., Briggs, P. R., Woodgate, W., Trudinger, C. M., Canadell, J. G., & Cuntz, M. (2018). A new version of the CABLE land surface model (subversion revision r4601) incorporating land use and land cover change, woody vegetation demography, and a novel optimisation-based approach to plant coordination of photosynthesis. *Geoscientific Model Development*, *11*(7), 2995–3026. https://doi.org/10.5194/gmd-11-2995-2018

Hong, C., Burney, J. A., Pongratz, J., Nabel, J. E. M. S., Mueller, N. D., Jackson, R. B., & Davis, S. J. (2021). Global and regional drivers of land use emissions in 1961–2017. *Nature*, *589*, 554–561. https://doi.org/10.1038/s41586-020-03138-y

Houghton, R. A. (2003). Revised estimates of the annual net flux of carbon to the atmosphere from changes in land use and land management 1850–2000. *Tellus B*, *55*(2), 378–390. https://doi.org/10.1034/j.1600-0889.2003.01450.x

Houghton, R. A., House, J. I., Pongratz, J., Van Der Werf, G. R., DeFries, R. S., Hansen, M. C., Le Quéré, C., & Ramankutty, N. (2012). Carbon emissions from land use and land-cover change. *Biogeosciences*, *9*(12), 5125–5142. https://doi.org/10.5194/bg-9-5125-2012

Houghton, R. A., & Nassikas, A. A. (2017). Global and regional fluxes of carbon from land use and land cover change 1850–2015. *Global Biogeochemical Cycles*, *31*(3), 456–472. https://doi.org/10.1002/2016GB005546

Huntzinger, D. N., Michalak, A. M., Schwalm, C., Ciais, P., King, A. W., Fang, Y., Schaefer, K., Wei, Y., Cook, R. B., Fisher, J. B., Hayes, D., Huang, M., Ito, A., Jain, A. K., Lei, H., Lu, C., Maignan, F., Mao, J., Parazoo, N., … Zhao, F. (2017). Uncertainty in the response of terrestrial carbon sink to environmental drivers undermines carbon-climate feedback predictions. *Scientific Reports*, *7*, 4765. https://doi.org/10.1038/s41598-017-03818-2

Hurtt, G. C., Chini, L., Sahajpal, R., Frolking, S., Bodirsky, B. L., Calvin, K., Doelman, J. C., Fisk, J., Fujimori, S., Goldewijk, K. K., Hasegawa, T., Havlik, P., Heinimann, A., Humpenöder, F., Jungclaus, J., Kaplan, J. O., Kennedy, J., Krisztin, T., Lawrence, D., … Zhang, X. (2020). Harmonization of global land use change and management for the period 850-2100 (LUH2) for CMIP6. *Geoscientific Model Development*, *13*(11), 5425–5464. https://doi.org/10.5194/gmd-13-5425-2020

Joos, F., Meyer, R., Bruno, M., & Leuenberger, M. (1999). The variability in the carbon sinks as reconstructed for the last 1000 years. *Geophysical Research Letters*, *26*(10), 1437–1440. https://doi.org/10.1029/1999GL900250

Joos, F., & Spahni, R. (2008). Rates of change in natural and anthropogenic radiative forcing over the past 20,000 years. *Proceedings of the National Academy of Sciences of the United States of America*, *105*(5), 1425–1430. https://doi.org/10.1073/pnas.0707386105

Kato, E., Kinoshita, T., Ito, A., Kawamiya, M., & Yamagata, Y. (2013). Evaluation of spatially explicit emission scenario of land use change and biomass burning using a process-based biogeochemical model. *Journal of Land Use Science*, *8*(1), 104–122. https://doi.org/10.1080/1747423X.2011.628705

Keeling, C. D., Piper, S. C., Bacastow, R. B., Wahlen, M., Whorf, T. P., Heimann, M., & Meijer, H. A. (2005). Atmospheric CO_2 and $^{13}CO_2$ exchange with the terrestrial biosphere and oceans from 1978 to 2000: Observations and carbon cycle implications. In J. R. Ehleringer, E. C. Thure, & M. D. Dearing (Eds.), *A history of atmospheric CO_2 and its effects on plants, animals, and ecosystems*. *Ecological studies* (Vol. *177*, pp. 83–113). Springer. https://doi.org/10.1007/0-387-27048-5_5

Knorr, W. (2009). Is the airborne fraction of anthropogenic CO_2 emissions increasing? *Geophysical Research Letters*, *36*(21), Article L21710. https://doi.org/10.1029/2009GL040613

Lawrence, D. M., Fisher, R. A., Koven, C. D., Oleson, K. W., Swenson, S. C., Bonan, G., Collier, N., Ghimire, B., Van Kampenhout, L., Kennedy, D., Kluzek, E., Lawrence, P. J., Li, F., Li, H., Lombardozzi, D., Riley, W. J., Sacks, W. J., Shi, M., Vertenstein, M., … Zeng, X. (2019). The community land model version 5: Description of new features, benchmarking, and impact of forcing uncertainty. *Journal of Advances in Modeling Earth Systems*, *11*(12), 4245–4287. https://doi.org/10.1029/2018MS001583

Le Quéré, C., Andrew, R. M., Canadell, J. G., Sitch, S., Korsbakken, J. I., Peters, G. P., Manning, A. C., Boden, T. A., Tans, P. P., Houghton, R. A., Keeling, R. F., Alin, S., Andrews, O. D., Anthoni, P., Barbero, L., Bopp, L., Chevallier, F., Chini, L. P., Ciais, P., … Zaehle, S. (2016). Global carbon budget 2016. *Earth System Science Data*, *8*(2), 605–649. https://doi.org/10.5194/essd-8-605-2016

Lienert, S., & Joos, F. (2018). A Bayesian ensemble data assimilation to constrain model parameters and land-use carbon emissions. *Biogeosciences*, *15*(9), 2909–2930. https://doi.org/10.5194/bg-15-2909-2018

MacFarling Meure, C., Etheridge, D., Trudinger, C., Steele, P., Langenfelds, R., Van Ommen, T., Smith, A., & Elkins, J. (2006). Law dome CO_2, CH_4 and N_2O ice core records extended to 2000 years BP. *Geophysical Research Letters*, *33*(14), Article L14810. https://doi.org/10.1029/2006GL026152

Magnani, F., Mencuccini, M., Borghetti, M., Berbigier, P., Berninger, F., Delzon, S., Grelle, A., Hari, P., Jarvis, P. G., Kolari, P., Kowalski, A. S., Lankreijer, H., Law, B. E., Lindroth, A., Loustau, D., Manca, G., Moncrieff, J. B., Rayment, M., Tedeschi, V., … Grace, J. (2007). The human footprint in the carbon cycle of temperate and boreal forests. *Nature*, *447*(7146), 848–850. https://doi.org/10.1038/nature05847

Mauritsen, T., Bader, J., Becker, T., Behrens, J., Bittner, M., Brokopf, R., Brovkin, V., Claussen, M., Crueger, T., Esch, M., Fast, I., Fiedler, S., Fläschner, D., Gayler, V., Giorgetta, M., Goll, D. S., Haak, H., Hagemann, S., Hedemann, C., … Roeckner, E. (2019). Developments in the MPI-M earth system model version 1.2 (MPI-ESM1. 2) and its response to increasing CO_2. *Journal of Advances in Modeling Earth Systems*, *11*(4), 998–1038. https://doi.org/10.1029/2018MS001400

Meiyappan, P., Jain, A. K., & House, J. I. (2015). Increased influence of nitrogen limitation on CO_2 emissions from future land use and land use change. *Global Biogeochemical Cycles*, *29*(9), 1524–1548. https://doi.org/10.1002/2015GB005086

Melton, J. R., Arora, V. K., Wisernig-Cojoc, E., Seiler, C., Fortier, M., Chan, E., & Teckentrup, L. (2020). CLASSIC v1.0: The open-source community successor to the Canadian land surface scheme (CLASS) and the Canadian terrestrial ecosystem model (CTEM) - part 1: Model framework and site-level performance. *Geoscientific Model Development*, *13*(6), 2825–2850. https://doi.org/10.5194/gmd-13-2825-2020

Meyer, W. B., & Turner, B. L. (1992). Human population growth and global land-use/cover change. *Annual Review of Ecology, Evolution, and Systematics*, *23*(1), 39–61. https://doi.org/10.1146/annurev.es.23.110192.000351

Millar, R. J., & Friedlingstein, P. (2018). The utility of the historical record for assessing the transient climate response to cumulative emissions. *Philosophical Transactions of the Royal Society A Mathematical Physical and Engineering Sciences*, *376*(2119), 20160449. https://doi.org/10.1098/rsta.2016.0449

Obermeier, W. A., Nabel, J. E. M. S., Loughran, T., Hartung, K., Bastos, A., Havermann, F., Anthoni, P., Arneth, A., Goll, D. S., Lienert, S., Lombardozzi, D., Luyssaert, S., McGuire, P. C., Melton, J. R., Poulter, B., Sitch, S., Sullivan, M. O., Tian, H., Walker, A. P., … Pongratz, J. (2021). Modelled land use and land cover change emissions—A spatio-temporal comparison of different approaches. *Earth System Dynamics*, *12*(2), 635–670. https://doi.org/10.5194/esd-12-635-2021

Peters, G. P., Le Quéré, C., Andrew, R. M., Canadell, J. G., Friedlingstein, P., Ilyina, T., Jackson, R. B., Joos, F., Korsbakken, J. I., McKinley, G. A., Sitch, S., & Tans, P. (2017). Towards real-time verification of CO_2 emissions. *Nature Climate Change*, *7*, 848–850. https://doi.org/10.1038/s41558-017-0013-9

Piao, S., Sitch, S., Ciais, P., Friedlingstein, P., Peylin, P., Wang, X., Ahlström, A., Anav, A., Canadell, J. G., Cong, N., Huntingford, C., Jung, M., Levis, S., Levy, P. E., Li, J., Lin, X., Lomas, M. R., Lu, M., Luo, Y., … Zeng, N. (2013). Evaluation of terrestrial carbon cycle models for their response to climate variability and to CO_2 trends. *Global Change Biology*, *19*(7), 2117–2132. https://doi.org/10.1111/gcb.12187

Pongratz, J., Dolman, H., Don, A., Erb, K.-H., Fuchs, R., Herold, M., Jones, C., Kuemmerle, T., Luyssaert, S., Meyfroidt, P., & Naudts, K. (2018). Models meet data: Challenges and opportunities in implementing land management in earth system models. *Global Change Biology*, *24*(4), 1470–1487. https://doi.org/10.1111/gcb.13988

Pongratz, J., Reick, C., Raddatz, T., & Claussen, M. (2008). A reconstruction of global agricultural areas and land cover for the last

millennium. *Global Biogeochemical Cycles*, *22*(3), article GB3018. https://doi.org/10.1029/2007GB003153

Pongratz, J., Reick, C. H., Houghton, R. A., & House, J. I. (2014). Terminology as a key uncertainty in net land use and land cover change carbon flux estimates. *Earth System Dynamics*, *5*(1), 177–195. https://doi.org/10.5194/esd-5-177-2014

Poulter, B., Frank, D. C., Hodson, E. L., & Zimmermann, N. E. (2011). Impacts of land cover and climate data selection on understanding terrestrial carbon dynamics and the CO_2 airborne fraction. *Biogeosciences*, *8*(8), 2027–2036. https://doi.org/10.5194/bg-8-2027-2011

Reay, D. S., Dentener, F., Smith, P., Grace, J., & Feely, R. A. (2008). Global nitrogen deposition and carbon sinks. *Nature Geoscience*, *1*(7), 430–437. https://doi.org/10.1038/ngeo230

Riahi, K., Schaeffer, R., Arango, J., Calvin, K., Guivarch, C., Hasegawa, T., Jiang, K., Kriegler, E., Matthews, R., Peters, G. P., Rao, A., Robertson, S., Sebbit, A. M., Steinberger, J., Tavoni, M., & van Vuuren, D. P. (2022). Mitigation pathways compatible with long-term goals, in IPCC, 2022. In P. R. Shukla, J. Skea, R. Slade, A. Al Khourdajie, R. van Diemen, D. McCollum, M. Pathak, S. Some, P. Vyas, R. Fradera, M. Belkacemi, A. Hasija, G. Lisboa, S. Luz, & J. Malley (Eds.), *Climate change 2022: Mitigation of climate change. Contribution of Working Group III to the sixth assessment report of the Intergovernmental Panel on Climate Change*. Cambridge University Press. https://doi.org/10.1017/9781009157926.005

Sellar, A. A., Jones, C. G., Mulcahy, J. P., Tang, Y., Yool, A., Wiltshire, A., O'Connor, F. M., Stringer, M., Hill, R., Palmieri, J., Woodward, S., de Mora, L., Kuhlbrodt, T., Rumbold, S. T., Kelley, D. I., Ellis, R., Johnson, C. E., Walton, J., Abraham, N. L., … Zerroukat, M. (2019). UKESM1: Description and evaluation of the UK earth system model. *Journal of Advances in Modeling Earth Systems*, *11*(12), 4513–4558. https://doi.org/10.1029/2019MS001739

Siegenthaler, U., & Oeschger, H. (1987). Biospheric CO_2 emissions during the past 200 years reconstructed by deconvolution of ice core data. *Tellus B: Chemical and Physical Meteorology*, *39*(1–2), 140–154. https://doi.org/10.3402/tellusb.v39i1-2.15331

Siegenthaler, U., & Sarmiento, J. L. (1993). Atmospheric carbon dioxide and the ocean. *Nature*, *365*, 119–125. https://doi.org/10.1038/365119a0

Sitch, S., Huntingford, C., Gedney, N., Levy, P. E., Lomas, M., Piao, S. L., Betts, R., Ciais, P., Cox, P., Friedlingstein, P., Jones, C. D., Prentice, I. C., & Woodward, F. I. (2008). Evaluation of the terrestrial carbon cycle, future plant geography and climate-carbon cycle feedbacks using five dynamic global vegetation models (DGVMs). *Global Change Biology*, *14*(9), 2015–2039. https://doi.org/10.1111/j.1365-2486.2008.01626.x

Smith, B., Wårlind, D., Arneth, A., Hickler, T., Leadley, P., Siltberg, J., & Zaehle, S. (2014). Implications of incorporating N cycling and N limitations on primary production in an individual-based dynamic vegetation model. *Biogeosciences*, *11*(7), 2027–2054. https://doi.org/10.5194/bg-11-2027-2014

Tian, H., Chen, G., Lu, C., Xu, X., Hayes, D. J., Ren, W., Pan, S., Huntzinger, D. N., & Wofsy, S. C. (2015). North American terrestrial CO_2 uptake largely offset by CH_4 and N_2O emissions: Toward a full accounting of the greenhouse gas budget. *Climate Change*, *129*(3), 413–426. https://doi.org/10.1007/s10584-014-1072-9

Van Der Werf, G. R., Randerson, J. T., Giglio, L., Collatz, G. J., Mu, M., Kasibhatla, P. S., Morton, D. C., Defries, R. S., Jin, Y., & Van Leeuwen, T. T. (2010). Global fire emissions and the contribution of deforestation, savanna, forest, agricultural, and peat fires (1997–2009). *Atmospheric Chemistry and Physics*, *10*(23), 11707–11735. https://doi.org/10.5194/acp-10-11707-2010

van Marle, M. J. E., van Wees, D., Houghton, R. A., Field, R. D., Verbesselt, J., & van der Werf, G. R. (2022). New land-use-change emissions indicate a declining CO_2 airborne fraction. *Nature*, *603*, 450–454. https://doi.org/10.1038/s41586-021-04376-4

Vuichard, N., Messina, P., Luyssaert, S., Guenet, B., Zaehle, S., Ghattas, J., Bastrikov, V., & Peylin, P. (2019). Accounting for carbon and nitrogen interactions in the global terrestrial ecosystem model ORCHIDEE (trunk version, rev 4999): Multi-scale evaluation of gross primary production. *Geoscientific Model Development*, *12*(11), 4751–4779. https://doi.org/10.5194/gmd-12-4751-2019

Walker, A. P., De Kauwe, M. G., Bastos, A., Belmecheri, S., Georgiou, K., Keeling, R., McMahon, S. M., Medlyn, B. E., Moore, D. J. P., Norby, R. J., Zaehle, S., Anderson-Teixeira, K. J., Battipaglia, G., Brienen, R. J. W., Cabugao, K. G., Cailleret, M., Campbell, E., Canadell, J. G., Ciais, P., … Zuidema, P. A. (2020). Integrating the evidence for a terrestrial carbon sink caused by increasing atmospheric CO_2. *New Phytologist*, *229*(5), 2413–2445. https://doi.org/10.1111/nph.16866

Walker, A. P., Quaife, T., van Bodegom, P. M., De Kauwe, M. G., Keenan, T. F., Joiner, J., Lomas, M. R., MacBean, N., Xu, C., Yang, X., & Woodward, F. I. (2017). The impact of alternative trait-scaling hypotheses for the maximum photosynthetic carboxylation rate (V_{cmax}) on global gross primary production. *New Phytologist*, *215*(4), 1370–1386. https://doi.org/10.1111/nph.14623

Wilson, A. T. (1978). Pioneer agriculture explosion and CO_2 levels in the atmosphere. *Nature*, *273*(5657), 40–41.

Woodwell, G. M., Hobbie, J. E., Houghton, R. A., Melillo, J. M., Moore, B., Peterson, B. J., & Shaver, G. R. (1983). Global deforestation: Contribution to atmospheric carbon dioxide. *Science*, *222*(4628), 1081–1086. https://doi.org/10.1126/science.222.4628.1081

Xu, L., Saatchi, S. S., Yang, Y., Yu, Y., Pongratz, J., Bloom, A. A., Bowman, K., Worden, J., Liu, J., Yin, Y., Domke, G., McRoberts, R. E., Woodall, C., Nabuurs, G.-J., de Miguel, S., Keller, M., Harris, N., Maxwell, S., & Schimel, D. (2021). Changes in global terrestrial live biomass over the 21st century. *Science Advances*, *7*(27), Article eabe9829. https://doi.org/10.1126/sciadv.abe9829

Yuan, W. P., Liu, D., Dong, W. J., Liu, S. G., Zhou, G. S., Yu, G. R., Zhao, T. B., Feng, J. M., Ma, Z. G., Chen, J. Q., Chen, Y., Chen, S. P., Han, S. J., Huang, J. P., Li, L. H., Liu, H. Z., Liu, S. M., Ma, M. G., Wang, Y. F., … Zhao, L. (2014). Multiyear precipitation reduction strongly decrease carbon uptake over North China. *Journal of Geophysical Research: Biogeosciences*, *119*(5), 881–896. https://doi.org/10.1002/2014JG002608

Yue, X., & Unger, N. (2015). The Yale interactive terrestrial biosphere model version 1.0: Description, evaluation and implementation into NASA GISS ModelE2. *Geoscientific Model Development*, *8*(8), 2399–2417. https://doi.org/10.5194/gmd-8-2399-2015

Zaehle, S., & Friend, A. D. (2010). Carbon and nitrogen cycle dynamics in the O–CN land surface model: 1. Model description, site-scale evaluation, and sensitivity to parameter estimates. *Global Biogeochemical Cycles*, *24*(1), Article GB1005. https://doi.org/10.1029/2009GB003521

SUPPORTING INFORMATION

Additional supporting information can be found online in the Supporting Information section at the end of this article.

How to cite this article: Dohner, J. L., Birner, B., Schwartzman, A., Pongratz, J., & Keeling, R. F. (2022). Using the atmospheric CO_2 growth rate to constrain the CO_2 flux from land use and land cover change since 1900. *Global Change Biology*, *28*, 7327–7339. https://doi.org/10.1111/gcb.16396